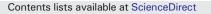
ELSEVIER



### Biochimica et Biophysica Acta

journal homepage: www.elsevier.com/locate/bbabio

# Reengineering cyt $b_{562}$ for hydrogen production: A facile route to artificial hydrogenases $\Rightarrow$



Dayn Joseph Sommer, Michael David Vaughn, Brett Colby Clark, John Tomlin, Anindya Roy<sup>1</sup>, Giovanna Ghirlanda \*

Department of Chemistry and Biochemistry, Box 871604, Arizona State University, Tempe, AZ 85287-1604, USA

#### ARTICLE INFO

Article history: Received 8 June 2015 Accepted 9 September 2015 Available online 12 September 2015

*Keywords:* Protein engineering Fuel production Cobalt catalysts Redox chemistry

#### ABSTRACT

Bioinspired, protein-based molecular catalysts utilizing base metals at the active are emerging as a promising avenue to sustainable hydrogen production. The protein matrix modulates the intrinsic reactivity of organometallic active sites by tuning second-sphere and long-range interactions. Here, we show that swapping Co-Protoporphyrin IX for Fe-Protoporphyrin IX in cytochrome  $b_{562}$  results in an efficient catalyst for photoinduced proton reduction to molecular hydrogen. Further, the activity of wild type Co-cyt  $b_{562}$  can be modulated by a factor of 2.5 by exchanging the coordinating methionine with alanine or aspartic acid. The observed turnover numbers (TON) range between 125 and 305, and correlate well with the redox potential of the Co-cyt  $b_{562}$  mutants. The photosensitized system catalyzes proton reductions. This article is part of a Special Issue entitled Biodesign for Bioenergetics – the design and engineering of electronic transfer cofactors, proteins and protein networks, edited by Ronald L. Koder and J.L. Ross Anderson.

© 2015 Elsevier B.V. All rights reserved.

#### 1. Introduction

Hydrogen, a carbon-neutral, energy-rich molecule, is an attractive alternative to fossil fuels, providing that new scalable and inexpensive methods to produce it become available [1,2]. Hydrogenases are able to carry out the reversible reduction of protons to hydrogen in neutral water and with low overpotentials, utilizing iron and/or nickel at the active site [3,4]. However, a number of drawbacks including oxygen sensitivity hamper their utilization, highlighting the need to investigate novel, robust catalysts [5–9]. In response to this challenge, several organometallic catalysts based on earth-abundant transition metals such as Fe, Ni, and Co have been reported [10–16]. With few notable exceptions, however, these systems are unable to work in water at mild conditions, and often require high overpotentials [11,17–19]. Further, obtaining catalytic efficiencies on par with natural hydrogenases remain a challenge.

Cobalt macrocyclic complexes are particularly attractive as hydrogen production catalysts because they can be easily modified, allowing for

(M.D. Vaughn), bcclark1@asu.edu (B.C. Clark), jjtomlin@asu.edu (J. Tomlin),

aroy10@uw.edu (A. Roy), gghirlanda@asu.edu (G. Ghirlanda).

fine control over redox properties, coupled with their unique ability to function under aerobic conditions [20-24]. Among these, cobalt porphyrins remain relatively unexplored despite their promising properties [25-28]. For example, a marked decrease in overpotential for electrochemical hydrogen evolution was observed in organic acids by a cobalt "hangman" porphyrin due to the inclusion of a carboxylic acid on the periphery of the catalyst [26]. Introducing ionic functionalities onto a Co(II) porphyrin scaffold permitted photoinduced hydrogen evolution in neutral water [27]. More recently, we and others have explored the substitution of CoPP(IX) for FePP(IX) in heme-binding peptides and proteins [29, 30]. One of the advantages of these systems is that the protein component is optimized to bind the porphyrin macrocycle and coordinate the metal via robust axial ligation by a single histidine residue, leaving the second axial position open for protonation. Substitution of cobalt for iron in microperoxidase-11 (CoMP11), a proteolytic fragment of cytochrome c, resulted in an electrocatalyst for proton reduction in water at pH 7, with an overpotential of 850 mV, turnover frequency of 6.7 s<sup>-1</sup>, and high Faradaic efficiency (>85% depending on conditions). In this construct, the CoPP(IX) is covalently linked to a helical fragment via thioether linkage to the porphyrin vinyl groups, and solvent exposed on the other side. These features are likely associated with loss of activity over a relatively short time (15 min).

Conversely, incorporation of CoPP(IX) into native, well-structured proteins is a developing approach to modulate the intrinsic activity of the catalytic center through second-sphere and long-range interactions, while shielding the macrocycle from inactivation through, for example, dimerization. Further, proteins provide rapid access to alteration of the

<sup>★</sup> This article is part of a Special Issue entitled Biodesign for Bioenergetics — the design and engineering of electronic transfer cofactors, proteins and protein networks, edited by Ronald L. Koder and J.L. Ross Anderson.

Corresponding author.

E-mail addresses: djsomme1@asu.edu (D.J. Sommer), mdvaughn@asu.edu

<sup>&</sup>lt;sup>1</sup> Present Address: Department of Biochemistry, Molecular Engineering and Sciences, University of Washington, Seattle, Washington, USA.

coordination sphere and long-range interactions through rational mutagenesis and/or directed evolution. We recently described the incorporation of CoPP(IX) into myoglobin obtaining a catalyst for hydrogen production both in electrocatalytic and photoinduced conditions at neutral pH. Photoinduced hydrogen production was sustained over 12 h, with TON of 518 [29,30]. Mutagenesis close to the porphyrin resulted in further increase in activity.

Here, we explore the effect of dual axial coordination to CoPP(IX) on catalytic activity, using the well characterized electron transfer protein cytochrome  $b_{562}$  (cyt  $b_{562}$ ) as scaffold [31–34]. This protein folds into an antiparallel four-helix bundle and binds a single heme within the hydrophobic core at one of the termini. In contrast to microperoxidase-11 and to myoglobin, cyt  $b_{562}$  coordinates heme at each of the two axial positions via methionine 7 and histidine 102, a motif found in a number of electron-transfer proteins [32,35-37]. We explored the effect of the coordination by comparing variants containing alanine, aspartic acid, or glutamic acid at the methionine's position. These latter variants were designed to place a proton relay in proximity of the cobalt center, mimicking the "hangman" moiety engineered by Nocera and coworkers [26]. This proton relay plays an important role in a variety of hydrogenase mimics, such as cobalt diimine-dioxime complexes and the nickel-based Dubois catalyst [17,24]. Rapid proton transfer to the active site is also required in [FeFe] hydrogenases, in which this function is enacted by the secondary amine moiety of the azadithiolate bridging ligand in the H-cluster [38,39]. We found that exchanging the second axial ligand to cobalt protoporphyrin IX in cyt  $b_{562}$  can modulate activity by a factor of 2.5.

#### 2. Materials and methods

#### 2.1. Mutant generation, purification, and porphyrin incorporation

Mutants were generated using Gibson assembly and sequenced directly in the pET30c + vector utilizing the T7 promoter sequence [40]. Verified mutants were transformed into a BL21(DE3) cell line and grown in 1 L of 2xTY media at 37 °C with shaking. Cells were induced with 1 mM IPTG at and OD<sub>600</sub> of 0.6 and cells were harvested after 4 h of expression. Cell pellets were suspended in 20 mM Tris-HCl, 1 mM DTT, 0.5 mM EDTA and lysed by multiple cycles of ultrasonication. The clarified lysate was brought to 75% saturation with solid ammonium sulfate and precipitated proteins were removed by centrifugation. The supernatant, containing the cytochrome mutants, was dialyzed against two changes of 10 mM Tris, pH 7.5 at 4 °C. Following dialysis, proteins were further purified via RP-HPLC utilizing a preparatory scale C18 column with a linear gradient from 100% A (99.9% water, 0.1% trifluoroacetic acid (TFA)) to 100% B (95% acetonitrile, 4.9% water, 0.1% TFA), followed by lyophilization to yield the pure apo-protein. Protein identities were confirmed via MALDI-TOF-TOF spectrometry and purity by C18 analytical analysis.

Purified proteins were reconstituted with Co-Protoporphyrin IX (CoPP(IX)) similarly to previously reported procedures [41,42]. Samples in 100 mM Tris, pH 8.5 were subjected to 50 M excess of DTT for 30 min, followed by a 50 M excess of CoPP(IX) for 1 h. Excess porphyrin was removed by subjecting protein to a PD10 desalting column (GE Healthcare) equilibrated in 50 mM Tris pH 7.5. Sample concentrations were determined via UV–Vis spectroscopy utilizing extinction coefficients of 8.6 mM<sup>-1</sup> cm<sup>-1</sup> (WT), 16.0 mM<sup>-1</sup> cm<sup>-1</sup> (M7A), 12.0 mM<sup>-1</sup> cm<sup>-1</sup> (M7E), and 9.9 mM<sup>-1</sup> cm<sup>-1</sup> (M7D) at the Soret. Protein was used immediately or frozen at -80 °C for future characterization.

#### 2.2. Porphyrin affinity determination

Apo and CoPP(IX)-bound proteins were characterized by UV–Vis spectroscopy. All spectra were recorded on a Varian 50 Cary Bio Spectrophotometer. Binding affinities to CoPP(IX) were determined by UV–Vis monitored titrations. Samples of the apo-protein in phosphate buffered saline were titrated by sequential addition of a Co(III)PP(IX) chloride stock in 0.1 M KOH and incubated for 10 min to allow for equilibration before data acquisition. The shift in the Soret peak of the bound state (425–430 nm) towards the unbound state (418 nm) was monitored as a function of porphyrin concentration, and data were analyzed with a simple 1:1 binding model.

#### 2.3. Circular dichroism spectroscopy

CD spectra were recorded on a JASCO J-815 spectropolarimeter in the range of 190–260 nm. Data were recorded every 1 nm and averaged over 3 scans. The concentration of apo and holo-peptides was kept at 10  $\mu$ M in 10 mM Tris, pH 7.5; measurements of the apo-peptide were carried out in the presence of an excess of TCEP. Thermal denaturation was performed by heating samples from 4 to 90 °C, monitoring loss of signal at 222 nm.

#### 2.4. Electrochemical methods

Electrochemical experiments were carried out using a CHinstruments 1242B potentiostat. For all electrochemical measurements, a three-electrode system was used: a 3-mm diameter glassy carbon working electrode with a surface area of  $0.28 \text{ cm}^2$ , platinum mesh counter electrode, and a saturated calomel reference electrode. Electrolyte solutions were degassed by incubation in a Coy anaerobic chamber for 2 days prior to use. Working electrodes were polished with 1 µm alumina for 5 min followed by 10 min of sonication. Electrodes were cleaned electrochemically by cycling 40 times between 1.2 and -1.2 V at 100 mV sec, followed by extensive washing with water, prior to use. Data were background subtracted using the SOAS software [43].

#### 2.5. Photoinduced H<sub>2</sub> production

Irradiation was performed using a Lumileds LXS8-PW27-0024(N) lamp, irradiating at a constant 1100 W/m<sup>2</sup> throughout the experiment. For each experiment, 1 mM Ru(Bpy)<sup>3+</sup>, 100 mM sodium ascorbate, and the desired catalyst were added to a 1 M potassium phosphate buffer at the appropriate pH. A 400  $\mu$ L total reaction volume was added to a custom made airtight 1 mm cuvette and degassed extensively with argon prior to illumination. During irradiation time course experiments, 100  $\mu$ L samples of gas taken from the headspace with a gas-tight syringe were injected directly for analysis with a SRI 310C gas chromatograph fitted with a 5 Å molecular sieve column and thermal conductivity detection. Calibration was achieved by injection of various volumes of a 1% H<sub>2</sub>, 99% N<sub>2</sub> gas mixture onto the GC.

An in-house developed continuous flow system was used for hydrogen detection in aerobic conditions similar to references [44,45]. An argon carrier stream flowing at 3 mL min<sup>-1</sup> delivered hydrogen produced in the reaction chamber to an in-line Figaro tin oxide hydrogen sensor (model TGS821, Figaro Engineering). The output of the hydrogen sensor was amplified using an instrumentation op-amp (Analog Devices, AD620AN). Illumination was achieved using a xenon arc lamp (Oriel 68,811 power supply with 66,028 lamp) at a total intensity of 1100 W/m<sup>2</sup>. For each experiment, 1 mM Ru(Bpy)<sup>2</sup>/<sub>3</sub><sup>+</sup>, 100 mM sodium ascorbate, and the desired catalyst were added to a 1 M potassium phosphate buffer and placed in a gas tight cuvette. Samples were equilibrated in the flowing gas for 30 min, followed by 30 min of baseline collection in the dark. Rates of hydrogen production were integrated to obtain moles of hydrogen produced, and utilized for calculation of final TON.

#### 3. Results and discussion

#### 3.1. Mutant design and binding to CoPP(IX)

We choose as scaffold for our investigation cyt  $b_{562}$  a 106-amino acid protein that folds into a stable, antiparallel four-helix bundle, and binds metallated protoporphyrin (IX) non-covalently through coordination by His107 and Met7 (Fig. 1) [34]. We characterized CoPP(IX)

Download English Version:

## https://daneshyari.com/en/article/1942094

Download Persian Version:

https://daneshyari.com/article/1942094

Daneshyari.com